On the Extraction of HCl and H2PtCl6 by Tributyl Phosphate: A Mode of Action Study

On the extraction of HCl and H_2PtCl_6 by tri-butyl phosphate: a mode of action study

Kirstian J. MacRuary,[1] Ross J. Gordon,[2] Richard A. Grant,[2] Stephen Woollam,[3] Ross J. Ellis,[4] Peter A. Tasker,[1] Jason B. Love[1] and Carole A. Morrison[1,*]

[1]School of Chemistry and EaStCHEM Research School, University of Edinburgh, David Brewster Road, Edinburgh, EH9 3FJ

[2]Johnson Matthey Technology Centre, Sonning Common, Reading, RG4 9NH

[3]Anglo American Technical Solutions, 8 Schonland Street, Theta, P.O. Box 106, Crown Mines, 2025, Johannesburg, South Africa.

[4]Oak Ridge National Laboratory, 1 Bethel Valley Road, Oak Ridge, TN, 37831 USA.

Keywords: solvent extraction, TBP, hydrochloric acid, platinum, micelle, molecular dynamics

Abstract

Combining computational modelling with experimental measurements has revealed the self-assembly of nano-aggregate structures in the transfer of HCl and $PtCl_6^{2-}$ from an aqueous phase into toluene by the common industrial extractant tri-butyl phosphate (TBP). Molecular dynamics simulations have been coupled to analytical measurements to provide an atomistic interpretation of the mode of action of TBP under 6 M and 10 M HCl conditions. The structures conform to reverse micelles, where the Cl^- or $PtCl_6^{2-}$ core is encapsulated by a hydration shell that acts as a mediating bridge to the electronegative oxygen atom in the TBP phosphate groups. For the 6 M HCl extraction model, the data support stable aggregates forming from 2-3 TBP molecules around one chloride anion if the number of water molecules encapsulating the chloride anion is no more than five; increasing the water content to ten molecules allows a fourth TBP molecule to coordinate. For the 10 M HCl extraction model, stable structures are obtained that conform to the empirical formula $(TBP.HCl.H_2O)_{3\text{-}5}$. At 6 M HCl, extraction of $PtCl_6^{2-}$ is achieved by encapsulation by four TBP molecules; the data for extraction at 10 M HCl indicate larger aggregates containing multiple $PtCl_6^{2-}$ anions are likely to be forming. In all cases, the hydrated core regions of the reverse micelles are considerably exposed. The diameters of the self-assembled

structures around chloride ions agree well with available literature data from small angle neutron scattering experiments.

Introduction

Tri-*n*-butyl phosphate (TBP, Figure 1) is a well-known compound employed in the recovery of inorganic acids (notably HCl, $HClO_4$ and HNO_3) and metals by solvent extraction from acidic media.[1-4] It is used extensively in the nuclear industry for the reprocessing of uranium, plutonium and thorium in the PUREX process,[5] and finds application as a modifier and solvent in many processes.[6-7]

This paper concerns the mode of action of TBP in the recovery of $PtCl_6^{2-}$ from aqueous HCl solutions of the type obtained by oxidative leaching of platinum group metal (PGM) concentrates.[8] In such a process $PtCl_6^{2-}$ is present in an acidic solution which contains other chloridometalate anions and a large excess of Cl^-.[9] In many cases the extraction of chloridometalates from acidic solutions can be represented by a simple ion pairing, to create charge-neutral assemblies which contain little or no water.[10-16] TBP can function as a 'solvating extractant',[17] bonding in either the inner or outer coordination sphere (or both) of a neutral metal complex, as in extraction of uranyl nitrate.[18] However, it can also operate by a different mechanism that involves formation of reverse micelle aggregates in which TBP behaves in a similar manner to a surfactant.[19] The reverse micelle structure is achieved by the polar head group of TBP associating with a water pool of the extracted anion(s) which is subsequently encapsulated by the aliphatic hydrophobic chains. These chains protrude into the organic solvent, essentially providing a layer between the water and the hydrophobic solvent. The formation of reverse micelles and, more generally third phases, by TBP has been studied extensively for nitrate-containing systems because of its importance in the separation and recovery of radionuclides.[20,21-22] The concept of a reverse micelle mode of action to transfer metal ions through water-oil interfaces by a range of surfactant ligands is now well established.[17, 23-28]

Given that the extraction of any chloridometalate anion will compete with a massive excess of chloride, it is important that the extraction behaviour of TBP with respect to hydrochloric acid is understood. Early work on the uptake of water and HCl by TBP (neat and in hydrocarbon solvents) is the subject of an excellent review

by Osseo-Asare.[7] Chiarizia *et al.*[21, 29] report small angle neutron scattering (SANS) data on HCl extractions by TBP into *n*-octane that provides a mechanistic explanation for third phase formation. Their data suggest the presence of reverse micelles which exist in solution as simple dimers that grow from aggregates containing two TBP molecules (when no HCl is present) to $(\{HCl\}_3\{H_2O\}_3 \cdot 7TBP)_{org}$, until the organic layer splits at 7.6 M HCl. This picture is somewhat at odds, however, with thermodynamic modelling of the TBP/HCl/water system by Lum *et al.*,[30] which predicted that the trisolvate species $(HCl\{H_2O\}_7 \cdot 3TBP)_{org}$ will dominate at low acid concentrations, while the di- and mono-solvates $(HCl\{H_2O\}_6 \cdot 2TBP)_{org}$ and $(HCl\{H_2O\}_3 \cdot TBP)_{org}$ become more prevalent as the acid concentration is increased. At HCl concentrations greater than 8 M water is lost from the organic phase and only a slight excess of water over HCl is observed, with a typical stoichiometry being $(\{HCl\}_{1.6}\{H_2O\}_{1.8} \cdot TBP)_{org}$.

While the extraction of metals by TBP has been the subject of many papers, there are gaps in knowledge which require attention. Its behaviour as an extractant in toluene appears not to have been reported and an in-depth investigation beyond the stoichiometries of components postulated to aggregate in the organic phase is missing. Information on the molecular structure, bonding, and the fundamental factors guiding the formation of the postulated macromolecular reverse micelles can be provided through molecular dynamics simulations, where the impact on the self-assembly of structures arising through systematic variation of the different components involved can be studied in depth. The focus of this paper is therefore to probe more deeply the behaviour of TBP for the extraction of HCl and $PtCl_6^{2-}$ into toluene. This study began with an analytical investigation to determine, as far as possible, the relative proportions of TBP, H_2O, HCl and $PtCl_6^{2-}$ that comprise the reverse micelles as a function of HCl concentration. These results were then used to guide computational modelling work, where self-assembly of reverse micelle structures were observed from components placed randomly in a toluene solvent box. Two HCl concentrations formed the basis for the computational investigation: 6 M HCl, since this is the acid concentration typically used for the commercial extraction of platinum group metals (PGMs) from HCl leach streams,[9] and 10 M HCl because the analytical measurements indicated a significant change in extractant behaviour at very high acid concentration.

Experimental and Computational Methods

Extraction set up. All solvents and reagents were used as received from Sigma-Aldrich, Fisher Scientific UK, Alfa Aesar, Acros Organics or VWR International. Deionised water was obtained from a Milli-Q purification system. Tri-*n*-butyl phosphate (TBP) was dissolved in toluene to create stock solutions of 0.5 and 1 M. The HCl concentration was varied from 2 M to 12 M. As HCl is known to promote hydrolysis of TBP,[31] contact and mixing of the equi-volume organic and aqueous phases was kept to a minimum (15 minutes, stirrer plate) before being physically separated. Any entrained water in the organic phase was subsequently removed either by phase separation paper (Whatman 1PS), centrifuge or sonicator.

Water and acid content analysis. Due to the high excess of chloride (2-12 M HCl) present in the (0.01 M) $PtCl_6^{2-}$ extractions, and as TBP will co-extract both these species, it was not possible to determine the levels of H_2O and H^+ associated with transport of just $PtCl_6^{2-}$ into the organic phase because the values are swamped by those involved in the extraction of HCl. Consequently, water and acid content analysis are only reported in the main text for the HCl extractions; data obtained in the presence of 0.01 M Na_2PtCl_6 can be found in the electronic supplement S1.2.

Water content of the organic phase pre- and post-extraction was measured by Karl Fischer titration, using a Metrohm 831 KF Coulometer charged with HYDRANAL® Coulomat AG reagent. Background levels of H_2O present in toluene following contact with 2-12 M HCl were also obtained to apply as a correction to the data when TBP was present.

The concentration of H^+ in the organic phase post-extraction was determined by making up 1 ml aliquots to 5ml in propanol, ensuring availability of sufficient volume to cover the Radiometer red rod REF201 universal electrode and Radiometer pHG 201/8 glass pH electrodes, against either standardised 0.1 M or 1 M NaOH solutions. The pH titrations were carried out using a Metrohm Titrando equipped with 800 Dosino dispensers.

Metal-content analysis. The concentration of Pt in the organic phase was determined using a Perkin Elmer Optima 5300DV inductively coupled plasma optical emission spectrometer. Sample solutions in 1-methoxy-2-propanol were taken up into a Gem Tip cross flow nebuliser and a Glass Cyclonic spray chamber at a rate of 2.0 mL min^{-1} and analysed using a RF forward power of 1500 W with argon gas flows of 20, 1.4 and 0.45 L min^{-1} for plasma, auxiliary and nebuliser flows, respectively. Resulting data were processed using WinLab32

for ICP-OES, version 3.0.0.0103. ICP-OES calibration standards for platinum in 10% hydrochloric acid were obtained from VWR International Ltd (UK).

Classical molecular dynamics simulations. All MD simulations were performed using the software package LAMMPS,[32] with the OPLS-AA force field[33] for all atom types with the exceptions of water (for which the TIP3P parameters were employed)[34] and $PtCl_6^{2-}$ (for which custom parameters were derived for the partial charge (q), Van der Waals well depth (ε) and collision diameter (σ), see electronic supplement S2.4). Partial charges (Mulliken) for TBP, $TBPH^+$ and H_3O^+ were calculated at the B3LYP/6-31G(d) level of theory using Gaussian09,[35] in a similar fashion to that reported by Cui[36] and Wipff.[37] Initial models were constructed using Packmol[38] to fit specific numbers of desired molecules randomly inside a cubic box of length 40 Å. Models comprised 3 to 6 TBP molecules, 0 to 10 H_2O molecules, 1 to 5 Cl^- anions, along with the appropriate number of charge balancing protons located on either TBP or H_2O molecules, and a sufficient number of toluene molecules to match the experimental solvent density at 298 K. Note the apparent low concentrations of components in the simulation box prevents multiple aggregates forming in the simulation, which would require a substantially larger periodic boundary unit cell. The xyz file was then converted into a LAMMPS data file using the VMD Topo tools.[39] Initial minimisation was carried out on all models by iteratively adjusting the atomic coordinates to reach a local potential energy minimum. Simulations were then run under NVT ensemble conditions to achieve equilibrium for approximately 0.05 ns (in integration time steps of 0.1 fs using the standard Velocity-Verlet algorithm), followed by simulations using the NPT ensemble for a minimum of 9 ns (integration time steps of either 0.5 or 1 fs), thermostated at room temperature and pressure using the Nosé-Hoover thermonstat/barostat system.[40-41] Further details can be found in the electronic supplement.

Results and Discussion

1. Extraction of HCl by TBP into toluene

Water content. As observed for other organic solvents,[31, 42] varying the HCl concentration in an aqueous phase in contact with toluene affects the amount of water which is transferred into the organic phase. For the system shown in Figure 2, which uses a 1 M solution of TBP in toluene, no third phase was formed. Below 6

M HCl only small amounts of water are extracted [see Figure 2(a)], but between 6 M and 12 M HCl the amount of water extracted increases to a maximum at *ca.* 10 M [HCl] and then decreases. Data points above 10 M HCl in Figure 2 were adjusted to account for changes in the relative volumes of the two phases by using a metal tracer in the aqueous phase and the amount of water transferred to the organic phase was corrected for background levels present in toluene (Electronic Supplement S1.1). Similarly shaped curves were obtained by Kertes[43] and Hardy[44] using 100% TBP although the absolute values differ (2M HCl extracted *ca.* 1.0 M H_2O and 9.0 M HCl extracted *ca.* 3.2 M H_2O). A study by Bach on 30% (v/v) TBP in xylene gives quantitative agreement with the data plotted in Fig 2(a).[42]

Acid content. Results for H^+ extraction are displayed in Figure 2(a), where minimal H^+ was detected in the organic phase upon contact with HCl below 6 M. Above 6 M HCl, $[H^+]$ rises in a linear fashion. Similar behaviour has been reported in other solvents.[31, 42-43,44]

Water:acid ratios in loaded organic phase. The ratio of H_2O to HCl measured upon extraction with varying initial HCl concentration in the aqueous phase is shown in Figure 2(b). The ratio falls rapidly, to levels of around 1:1 at 9–10 M HCl, dropping further thereafter. Two key concentrations of HCl are the focus of discussion below: 6 M HCl, which is the acid concentration typically used in the extraction of PGMs from HCl-leach streams,[9] where our analysis suggests $HCl\{H_2O\}_{2.5}$ [Figure 2(b) red point], and 10 M HCl, where the concentration of H_2O detected in the organic phase reached a maximum, and our analysis suggests $HCl\{H_2O\}$. Our data match very closely the report by Lum *et al* for high acid extraction[30] but our lower acid extraction model suggests a notably less hydrated core, which may arise due to the different solvents used.

2. Extraction of $PtCl_6^{2-}$ by TBP into toluene

$PtCl_6^{2-}$extraction. The ability of TBP solutions in toluene to extract $PtCl_6^{2-}$ as a function of TBP and HCl concentration is summarised in Figure 3(a). Extractant performance of TBP is highly dependent on HCl concentration. Data reported here are comparable with those reported by Sun *et al*.[45] For extractant solutions containing more than 1 M TBP the platinum-loading decreases significantly as the initial concentration of HCl in the aqueous feed solution is increased. This behaviour is typical for extraction of chloridometalates which are competitively extracted alongside chloride anions.[9]

Slope analysis. TBP:$PtCl_6^{2-}$ ratios pertaining to the extractions at 6 M and 10 M HCl were obtained from analysis of the distribution coefficient, *D*, where $D = [Pt]_{org}/[Pt]_{aq}$, and the gradient of a plot of log *D* against log [TBP] gives the ratio of the two components in the extracted species. The results of these analyses are given in Figure 3(b,c). At 10 M HCl the straight line fit ($R^2 = 0.992$) suggests that two TBP molecules are associated with each $PtCl_6^{2-}$ ion in the organic phase. The curved form of the plot at 6M HCl indicates that the extraction process involves the formation more than one type of assembly in the organic phase. The curved form is not associated with experimental errors as the Pt content of each phase was estimated to be subject to ≤ 3% error and no third phase was detected. Whilst, as might be expected for a complex system in which aggregation of species in the organic phase is possible, the log D plots did not provide evidence for the formation of a single species under all conditions, they proved useful in providing guidelines for the range of stoichiometries (i.e. 2-5 TBP to $PtCl_6^{2-}$) which should be considered in modelling the formation of reverse micelle type assemblies.

3. Molecular dynamics simulations

3.1 Models for extraction of Cl^- from 6 M HCl. MD simulations were performed to establish the maximum number of TBP molecules that can assemble around one Cl^- anion in the presence of a small amount of water. The number of water molecules was varied (0, 5 or 10) in order to directly assess the impact of water in the assemblies thus formed. Note that care needs to be taken not to over interpret the observations from the modelling work as, unlike the solvent extraction experiment, the periodic boundary condition model used does not have an interface to an aqueous layer. As such, any water molecules present in the simulation cell will naturally gravitate to the anion, whereas in the real extraction the polar environment of the aqueous phase may act as a stronger attractant than the organic phase. To establish charge neutrality, an H^+ counter ion must be present, which can be attached to either a TBP molecule or a H_2O molecule. Whilst it is more likely that the proton resides on a water molecule (and in all likelihood hops between water molecules)[46] we pursued both options in this work, as geometry optimisation calculations [M06/6-31G(d)] on the system TBP….H_3O^+ resulted in the proton 'hopping' to the TBP, leaving a hydrogen bound water molecule, indicating that, in the gas phase at any rate, $TBPH^+$ is a stable species. Also, within a small reverse micelle containing only a few "structured" water molecules H-bonded to an anion which will reduce their basicity, the option of a proton residing on a TBP molecule might be more favourable than in a bulk phase.

In all simulations, a single aggregate was observed to form spontaneously, where the Cl^- anion was surrounded by a water shell, which in turn was surrounded by a TBP shell (see Figures 4 and 5). The structure therefore conforms to what could be regarded as a reverse micelle. Regardless of whether the counter cation is H_3O^+ or $TBPH^+$, it quickly became apparent that whilst the maximum number of TBP molecules that could assemble around the chloride anion was four, assemblies containing two or three TBP molecules were far more common [see electronic supplement S2.1]. This finding is in line with the thermodynamic modelling, which suggested a ratio of HCl: 3TBP at low acid concentration.[30] The simulations also appear to support the levels of micelle hydration identified by the Karl-Fischer titrations: in the complete absence of water, the number of associated TBP molecules most often found was just two, while increasing the number of water molecules (to ten) usually permitted four TBP molecules to aggregate. This suggests that one function of the water molecules is to provide a larger volume around the chloride anion with which extractant molecules can interact.

For the MD simulations comprising $TBPH^+$ as the counter ion, simple electrostatics would predict this ion to lie closer to the Cl^- anion than neutral TBP molecules, and this indeed was always found to be the case [Figure 4(b) and electronic supplement S2.1]. The $Cl^{-}\cdots O(TBPH^+)$ distance, 3.05 Å, is recorded as a sharp peak on the g(r) plot, which indicates that this is a strong interaction that varies little throughout the simulation. In contrast, the $Cl^{-}\cdots O(TBP)$ distances form a broader continuum, centred around 3.6 Å. Optimisation of the aggregate (M06/6-31G(d) level, gas phase model) gave similar distances: $Cl^{-}\cdots O(TBPH^+)$ = 2.8 Å, $Cl^{-}\cdots O$ (TBP) = 3.0 Å, which lends credence to the force field parameters used. The water molecules are most commonly located between the chloride ion and the TBP molecules, but never disrupt the $Cl^{-}\cdots O(TBPH^+)$ ion pair. The model that emerges is thus one where the water molecules act as mediating bridges between the negatively charged chloride ion and electronegative oxygen atoms in the P=O group of the TBP molecules, whilst the positively charged $(BuO)_3P{=}OH^+$ unit forms the ion pair contact, as summarised in Figure 4(c).

Information on the size of the reverse micelle formed can be obtained from atomic density plots [Figure 4(d)], where the coordinates of all atoms bar the toluene solvent molecules from each frame of the MD simulation

are shifted to ensure that the centre of mass lies at the centre of the box, and the positions of atom types are binned to generate probability distribution plots. The chloride anion does not sit at the centre of mass, implying mobility of the anion within the aggregate towards the $TBPH^+$ cation and/or a shifting centre of mass due to flexibility of the hydrocarbon chains on the TBP molecules. The probability density plots allow the sizes of each of the approximately Gaussian concentric shells making up the aggregate to be determined. This gives a maximum radius of 5 Å for the chloride core, which rises to 8-10 Å when the water and TBP layers are included. This closely matches the diameter (*ca.* 18 Å) reported by small angle neutron and X-ray scattering (SANS and SAXS) for aggregates formed on extraction of HCl by TBP into *n*-dodecane[20] and *n*-octane.[47]

Switching the counter cation to H_3O^+ has a marked effect on the structures obtained. While the most commonly observed aggregates again contain two or three TBP molecules (Electronic Supplement S2.1), the shape of the aggregate changes from an approximately spherical arrangement to a more prolate structure [Figure 5(a)]. Sharp peaks on the g(r) $Cl^-\ldots O(H_2O/H_3O^+)$ plot [Figure 5(b)] show the formation of a water shell around the chloride ion, with two distinct features at 2.95 and 3.25 Å which are consistently present, regardless of the number of TBP molecules included in the simulation box. The schematic diagram in Figure 5(c) shows that the short contact distance relates to binding of the charged hydronium ion, which in turn 'pins' two TBP molecules to the hydrated core, while the longer distance relates to the neutral H_2O molecules which also surround the chloride anion. The atomic density plot [Figure 5(d)] appears to suggest a lack of coherent structure, with each component equally dispersed within the aggregate, in marked contrast to that described from the simulation where the counter ion is $TBPH^+$. However, as this analysis is essentially a histogram of atomic positions as a function of distance from the centre of mass, averaged over many trajectory snapshots, it will not perform well for randomly orientated structures that deviate substantially from a sphere.

To establish how well TBP molecules encapsulate a hydrated chloride anion, 50 random frames were selected from the production run trajectories that contained three TBP molecules, five H_2O molecules and one Cl^- ion, for both the $TBPH^+$ and H_3O^+ counter ion simulations. The amount of core region exposed to the surrounding solvent (the percentage core exposure) can be calculated via a Monte Carlo script that shoots a probe point from 10,000 random positions on the surface of a sphere (which is centred on the chloride ion and which

completely encapsulates the aggregate) towards the chloride ion and counts what atom type it hits first on its path; the number of times the probe hits an atom in a water molecule or a Cl^- anion (represented as spheres of appropriate van der Waal radii) is then recorded as a percentage of the total probe runs. Low core exposure values therefore indicate that the water molecules are less exposed. The analysis was repeated for each of the 50 random frames, which allows an average and standard deviation to be reported (see Table 1) and reveals core exposure values of 53(2) % when the counter ion in the simulation was $TBPH^+$, compared to 57(5) % for counter ion H_3O^+. In both cases the core is therefore relatively exposed.

The picture that emerges from the computational modelling work is one where stable assemblies readily form that comprise three TBP molecules to one chloride anion if the number of water molecules included in the aggregate is below ten, which finds good agreement with the conclusions reached by Lum *et al*.[30] The size distribution obtained for the more spherical aggregates formed when the counter ion is $TBPH^+$ is also in excellent agreement with SANS and SAXS measurements.[20, 47] Turning to the details that the atomistic simulations can provide, the new insight gained relates to direct observation of water molecules acting as a mediating shell between $(n\text{BuO})_3P^{\delta+}=O^{\delta-}$ and Cl^-, which would otherwise be a repulsive interaction. The observed structures also have relatively exposed core regions, indicating that rather 'leaky' reverse micelles have formed. If the TBP carries the proton the structure formed is essentially a reasonably spherical hydrated ion-pair, with a well-defined water shell; if the proton shifts to a water molecule the structure becomes markedly more prolate.

3.2 Models for extraction of Cl^- from 10 M HCl. The analytical measurements reported in Figure 2 suggest a substantial change in mode of action for extraction of HCl with increasing acid concentration, with likely ratios of core components fitting the empirical formula $(H_2O.HCl)_y$ at 10 M HCl, in line with the thermodynamic modelling work of Lum *et al*.[30]

MD simulations were explored with equimolar quantities (3, 4 and 5 molecules) of TBP, H_2O and Cl^-, with counter ions of either $TBPH^+$ or H_3O^+, as before. In all simulations, a single aggregate was observed to form spontaneously, containing all of the TBP present (Electronic Supplement S2.2). The nature of the counter ion was again observed to have a marked effect on the structures formed, as demonstrated by the atom probability

plots in Figure 6, which show a noticeably more diffuse water structure when protonated. The simulations with $TBPH^+$ counter ions return aggregates of very similar size for structures containing 3-5 Cl^- ions, with encapsulated hydrated chloride core diameters of about 15 Å, which rises to around 20 Å including the TBP shell. Aggregates appear to be larger (diameters ca. 25 Å) when the counter ion is H_3O^+, and the atom probability plots show evidence of layered structures for cores comprising 4 or 5 Cl^- ions, which suggests a return to a more spherical structure. Chiarizia *et al*., have performed SANS measurements for TBP extraction of HCl into *n*-octane, and concluded that upon increasing acid concentration the aggregates swell by about 4.5 Å, and have polar core diameters of around 10–15 Å.[48] This compares favourably with the results obtained in our study.

Analysis of individual g(r) plots for the $(TBP.HCl)_4$ system (Figures 7 and 8) show in more detail the architecture of the core region: when the counter ion is $TBPH^+$ the maximum probability $Cl^{-}\cdots Cl^-$ distance is greater (*ca*. 4.25 Å) than when the counter ion is H_3O^+ (*ca*. 4.05 Å). The H_2O molecules in the former simulation are more closely packed than the H_3O^+ ions in the latter ($O\cdots O$ distances *ca*. 3.0 Å *vs*. 4.5 Å), an observation also noted from the atom probability plots in Figure 6. In essence this suggests a model comprising a hydrated chloride core where the Cl^- ions protrude when surrounded by a charged $TBPH^+$ shell, or the H_3O^+ cations protrude when attracted by the $P{=}O^{\delta-}$ group from a shell of charge-neutral TBP molecules. These structural characteristics are displayed schematically alongside the corresponding g(r) plots in Figures 7 and 8. Other noteworthy features of the g(r) plots are that Cl^- binds tightly to both H_3O^+ and $TBPH^+$ (sharp peaks), but whilst H_3O^+ also binds tightly to TBP (2.55 Å), H_2O appears to cluster more loosely around $TBPH^+$ ions. The tight-binding of H_3O^+ is mirrored in RMSD plots, which suggest that the $(H_3O^+.Cl^-)_{3-5}$ core is always more rigid than a $(H_2O.Cl^-)_{3-5}$ core (Electronic supplement, S2.2). Interestingly, a super-concentrated HCl water pool has been reported in the extraction of $PtCl_6^{2-}$ by a tertiary amine ligand in a reverse micelle mechanism.[49]

The core exposure measurements (Table 1), averaged over 50 snapshots selected at random from each MD production run trajectory, suggest the hydrated chloride core is shielded more effectively as the number of bound TBP surfactant molecules rises. It is tempting to attribute the relatively exposed hydrated cores to the

cause of third phase formation reported for TBP in solvent extraction processes under high acid or high metal loading conditions,[29] as aggregates may merge to combine exposed water pools, which would lead to larger assemblies carrying increasing amounts of water into the organic phase, resulting in the solvent interface breaking down. SANS measurements for extractant aggregation have typically been interpreted using the Baxter model of sticky hard spheres,[50] suggesting the existence of a short-range attractive potential between aggregates. Recent measurements by diffusion NMR spectroscopy on the extraction of $Zr(NO_3)_4$ by TBP,[22] have suggested that long-range repulsive interactions can also arise if the negatively charged core region is exposed; the modelling work performed here clearly supports a fluxional aggregate with significantly exposed core region.

Finally, we explored the effect of increasing the number of TBP molecules (up to eight) available to aggregate around a core of four Cl^- ions and four water molecules. Regardless of the nature of the counter cation, results indicate that it is unusual for more than four TBP molecules to interact with the core (electronic supplement S2.3), which is at odds with Chiarizia's high acid concentrations model (which has seven TBP molecules around a $(H_3O^+.Cl^-)_3$ core),[29] but does support the thermodynamically-postulated structures by Lum *et al*, which propose a lower chloride to TBP ratio at high acid concentration.[30]

3.3 Models for extraction of $PtCl_6^{2-}$ from 6 M HCl. Given that the Karl Fischer titrations could not be used to ascertain the quantity of water involved in the extraction species (due to the simultaneous extraction of Cl^-, which pulls substantial quantities of water into the organic phase, and is present in vast excess compared to $PtCl_6^{2-}$, see electronic supplement S1.2), in this work the impact of any water associated with the aggregates has instead been probed *via* computational modelling. The number of TBP molecules present in the toluene simulation box was varied from four to six, and the number of water molecules present was either 0, 2, 5 or 10. With the anion acting as the nucleation point now carrying a 2– charge, two cations are now need to ensure neutrality. In this study, the impact of assigning the counter ions as $TBPH^+$ or H_3O^+ was assessed as these mark the two extreme cases. Note also that a reverse micelle could contain both $PtCl_6^{2-}$ and Cl^-, but we have not explored this possibility here.

With the counter ions set to $TBPH^+$, modelling indicates that four TBP molecules can be comfortably accommodated around a single $PtCl_6^{2-}$ anion in the absence of any water molecules (see electronic supplement S2.5), which is in line with the slope analysis measurements reported above. Increasing the number of TBP molecules to six indicated that a fifth molecule can be incorporated into an aggregate, but only transiently. Introducing five H_2O molecules into the simulation box gives a similar result: the most common number of coordinating TBP molecules is still four. Increasing still further (to ten H_2O) increases the frequency of a fifth interacting TBP molecule, but this is still in a transient fashion. In contrast, if both counter ions are set to H_3O^+ it is only when a total of ten water molecules are present that association of four neutral TBP molecules can be maintained (electronic supplement S2.5). Core exposure analysis indicates that around 20% of the water pool is exposed in these reverse micelles (Table 1).

As expected on the basis of electrostatics, Pt…O($TBPH^+$) distances are shorter than Pt…O (TBP) distances [*ca.* ca. 4.0 and 5.3 Å in the absence of any water (see electronic supplement S2.5), rising to *ca.* 4.35 and 5.85 Å, respectively when ten water molecules are present; the most probable Pt...O(H_2O) distance is centred around 4.45 Å, indicating that if any water molecules are present they reside in the same coordination shell as the head-group of the $TBPH^+$ [see Figure 9(a) and 9(b)]. The atomic density plots [Figure 9(c)] show that in the presence of water a spherical structure is seen comprising distinct shells with the $PtCl_6^{2-}$ unit found close to the centre of mass of the aggregate. The diameter of the aggregate including the TBP shell is approximately 25 Å [Figure 9(c)], which decreases slightly on removal of the water molecules (electronic supplement S2.5). Thus, it is clear that these assemblies are notably larger than those formed on extraction of single chloride ions. As with the chloride extraction models discussed earlier, if water molecules are present they effectively negate repulsive interactions between the negatively charged anion and the negative dipoles on the oxygen atoms of the surfactant TBP molecules through hydrogen bonding. One notable difference compared to the chloride reverse micelle model is that water molecules are more likely to disrupt the $TBPH^{+\cdots}PtCl_6^{2-}$ 'ion-pair' interactions, which presumably relates to the more diffuse nature of the larger anion. The loose-binding of the water molecules to the anion is neatly captured in the g(r) plots [contrast $PtCl_6^{2-}$…H_2O in Figure 9(a) against the corresponding more tightly bound Cl^-…H_2O in Figure 5(b)].

The analogous data obtained for the $PtCl_6^{2-}$ extraction model when the counter ions were set to H_3O^+ are presented in Figure 10. Both H_3O^+ counter ions coordinate firmly to opposing octahedral faces of the $PtCl_6^{2-}$ anion and act to 'pin' two TBP molecules in place, with the remaining eight water molecules forming a hydrogen-bonded cluster close to the $PtCl_6^{2-}$ anion [see Figure 10(b)]. This assembly forms early in the production run trajectory, with the only variant being the migration of one TBP molecule along one or two positions of the water cluster. The atom probability distribution plot shown in Figure 10(c) indicates a highly structured reverse micelle structure has formed, which is a little larger than the structure formed by the $TBPH^+$ counter ions.

4.2 Models for extraction of $PtCl_6^{2-}$ from 10 M HCl. Evidence from the slope analysis measurements suggest a change in the mode of action behaviour from $(PtCl_6\{H_3O\}_2\{H_2O\}_x{\cdot}TBP_4)_{org}$ at 6 M HCl to $(PtCl_6\{H_3O\}_2\{H_2O\}_x{\cdot}TBP_2)_{org}$ at 10 M HCl. From the modelling work reported in the previous section it is apparent that four TBP molecules can be readily accommodated around a solvated $PtCl_6^{2-}$ core, thus the only way to drop the $PtCl_6^{2-}$:TBP ratio is to explore higher order aggregates containing multiple $PtCl_6^{2-}$ anions, or that the mode of action is changed to a simple ion pairing. This latter option seems unlikely from the modelling work as in the presence of excess TBP it is rare for the coordination number to drop below four (electronic supplement, S2.5). For the former option, the models quickly become large, however, and in the absence of any further experimental data to establish the size of aggregates formed, a preliminary calculation was performed on a simulation box containing two $PtCl_6^{2-}$ anions only with four $TBPH^+$ and two TBP molecules (*i.e.* two TBP molecules potentially in excess) and six water molecules (arbitrary choice). Whilst an aggregate quickly formed, it did not conform to the sought-after $PtCl_6^{2-}$:2TBP ratio, as two of the $TBPH^+$ ligands were observed to straddle the two $PtCl_6^{2-}$ anions, which in turn were each bound by one $TBPH^+$ and one TBP unit. Thus the number of interacting TBP ligands per $PtCl_6^{2-}$ remained four. This suggesting that higher order aggregates, containing three or more $PtCl_6^{2-}$ anions need to be explored. The possibility that two $PtCl_6^{2-}$ anions can be extracted by two TBP with two H_3O^+ counter ions cannot be ruled out, nor the possibility that $PtCl_6^{2-}$ and Cl^- are co-extracted in the same assembly. It is therefore apparent that further experimental investigation is required to guide the computational study any further.

Conclusions

This paper has probed TBP mode of action in the extraction of Cl^- and $PtCl_6^{2-}$ from acidic chloride solutions. To the best of our knowledge the experimental results presented are the first report of TBP performance in toluene, and suggest the absence of any third phase formation, which has hampered studies in other hydrocarbon solvents. Classical molecular dynamics simulations performed on models constructed from experimentally derived ratios of HCl and H_2O resulted in the spontaneous formation of assemblies that can be described as reverse micelles. The diameter of chloride-containing micelles (16-18 Å for the 6 M HCl extraction model, rising to *ca*. 20-22 Å for the models explored for the 10 M HCl extraction model) match well with data reported from SANS experiments, giving validity to the structures described. Modelling suggests that the experimental component ratios expressed at 6 M HCl can be best accommodated by a structure derived from two to three TBP molecules interacting with one chloride anion, which is surrounded by no more than ten water molecules. For the 10 M HCl extraction data, modelling indicates that reverse micelles containing multiple chloride anions (we explored up to five), with a matching ratios of TBP and water molecules, all gave stable assemblies. For $PtCl_6^{2-}$extraction, slope analysis indicated that more than one type of assembly can form in the organic phase and that four or more TBP molecules can be associated with each $PtCl_6^{2-}$ at 6 M HCl, which was matched by the computational modelling. At 10 M HCl the experimental data indicated that the number of coordinating TBP molecules to each $PtCl_6^{2-}$ falls to two, suggesting the formation of a larger aggregate which the modelling work suggests will contain more than two $PtCl_6^{2-}$ ions. The role of water in the extraction of $PtCl_6^{2-}$ is unclear, but it appears to be less important than for the extraction of Cl^-, with a simulations devoid of any water molecules still capable of attracting the expected four TBP molecules as observed experimentally under 6M HCl extraction conditions. The chloridoplatinate-containing micelles are significantly larger than the chloride-containing structures.

The MD simulations applied in this work prevent the spontaneous 'hopping' of H^+ ions between molecular units, and so by pursuing both H_3O^+ or $TBPH^+$ as counter ions the two extremes of behaviour have been explored. Results indicate that whilst both options result in stable assembly formation, those constructed from H_3O^+ counter ions give more rigid hydration core structures. This supports the concept of a highly concentrated acidic core, as suggested by earlier literature reports.[49] The modelling work also reveals that the

observed levels of TBP aggregation result in structures with relatively exposed hydrated core regions, which provides insight into why third phase formation occurs in solvent extraction processes.

Acknowledgements

KJM acknowledges JM and AngloPlatinum for PhD funding and The University of Edinburgh ECDF and EaStCHEM RCF facilities for access to high performance computing resources. We also thank Dr J. Bradley-Shaw and Mr. Innis Carson (University of Edinburgh) for helpful discussions on LAMMPS simulations and data interpretation.

Table 1 Percentage core exposure for aggregates formed in the MD simulations

Aggregate	Counter ion	
	$TBPH^+$	H_3O^+
3TBP, Cl^-, $5H_2O$	53(2)	57(5)
4TBP, $4Cl^-$, $4H_2O$	51(2)	45(1)
4TBP, $PtCl_6^{2-}$, 10 H_2O	19(1)	22(1)

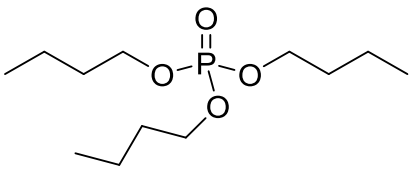

Figure 1 Tri-n-butyl phosphate (TBP)

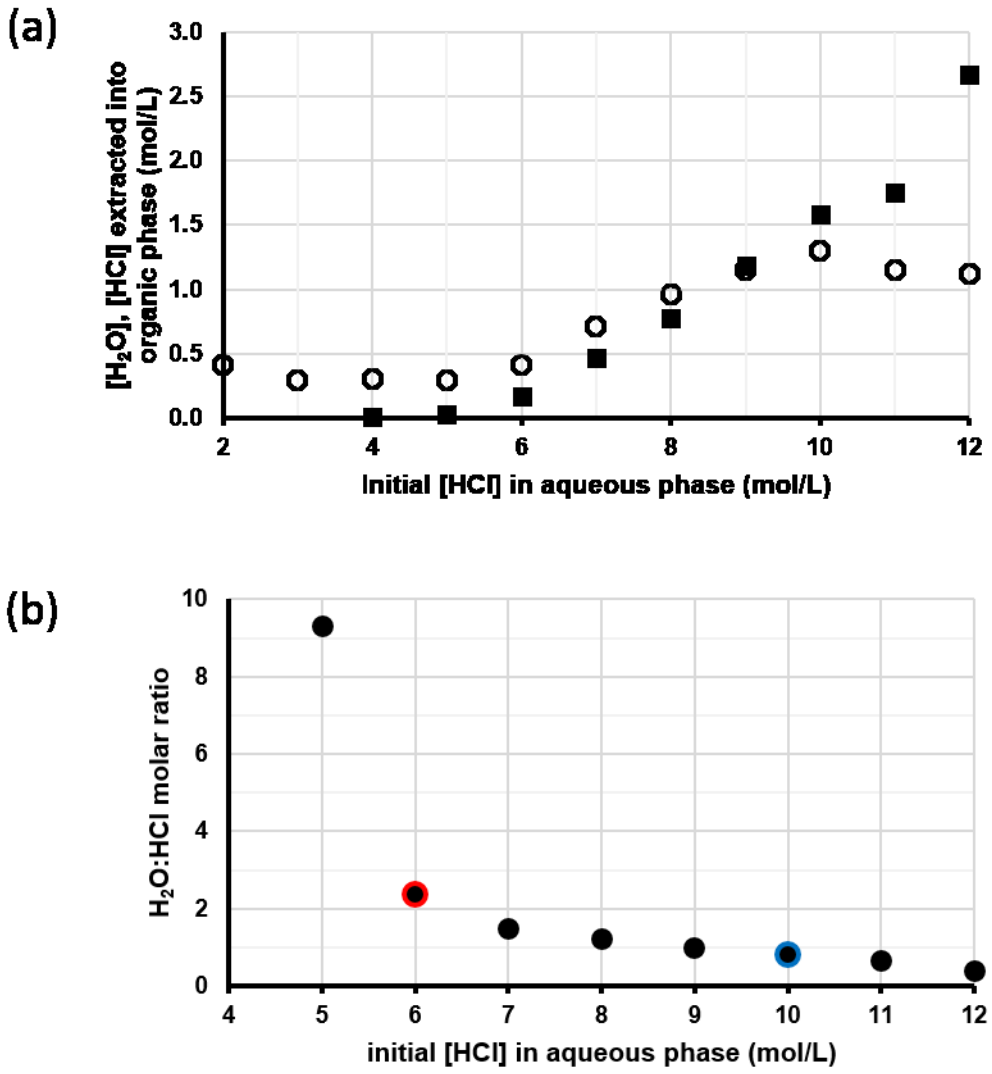

Figure 2 Measured concentrations of (a) H_2O (open circles) and HCl (filled squares) in a 1 M solution of TBP in toluene after contacting with an equal volume of an aqueous solution of HCl, as a function of $[HCl]_{initial}$. Background levels of water present in toluene in absence of TBP have been subtracted. (b) Molar ratio of H_2O:HCl in a 1 M TBP toluene solution after contacting with an equal volume of aqueous HCl, as a function of $[HCl]_{initial}$.

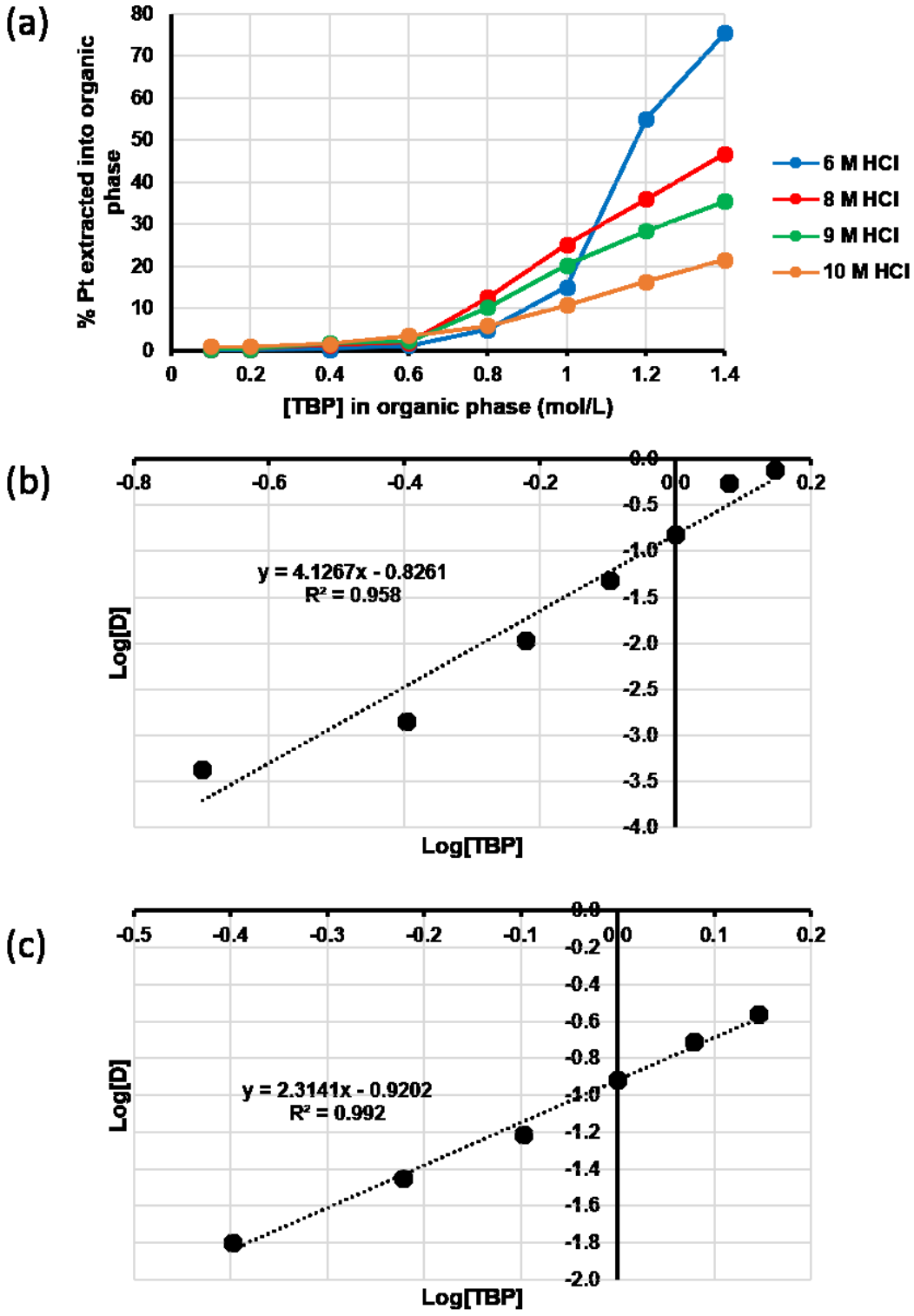

Figure 3 (a) %Pt extracted into toluene as a function of $[TBP]_{org}$ and $[HCl]_{initial}$; Log D_{Pt} plots for extraction by toluene solutions of varying [TBP] from 0.01 M $PtCl_6^{2-}$ aqueous solutions containing (b) 6 M HCl or (c) 10 M HCl.

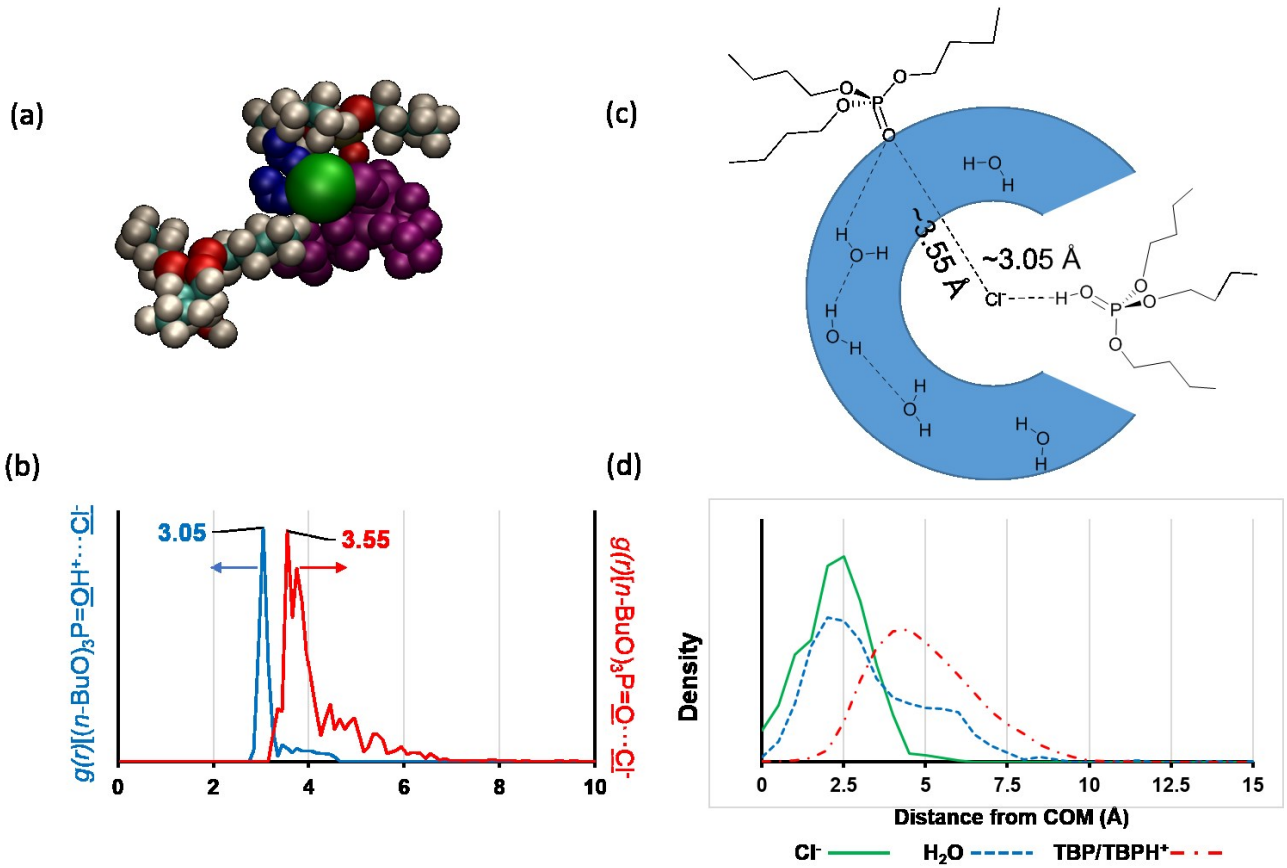

Figure 4 (a) VDW representation of aggregate formed with 3 TBP molecules (two are bound, the protonated molecule is shown in purple and water molecules in dark blue) around a core of $(H_2O)_5Cl^-$, (b) g(r) distance plots detailing the probability distribution of distances for the underlined atoms over the production run dynamics, (c) schematic diagram showing the main structural features of the aggregate, and (d) atom probability plots showing the concentric shell structure with respect to the aggregate centre of mass.

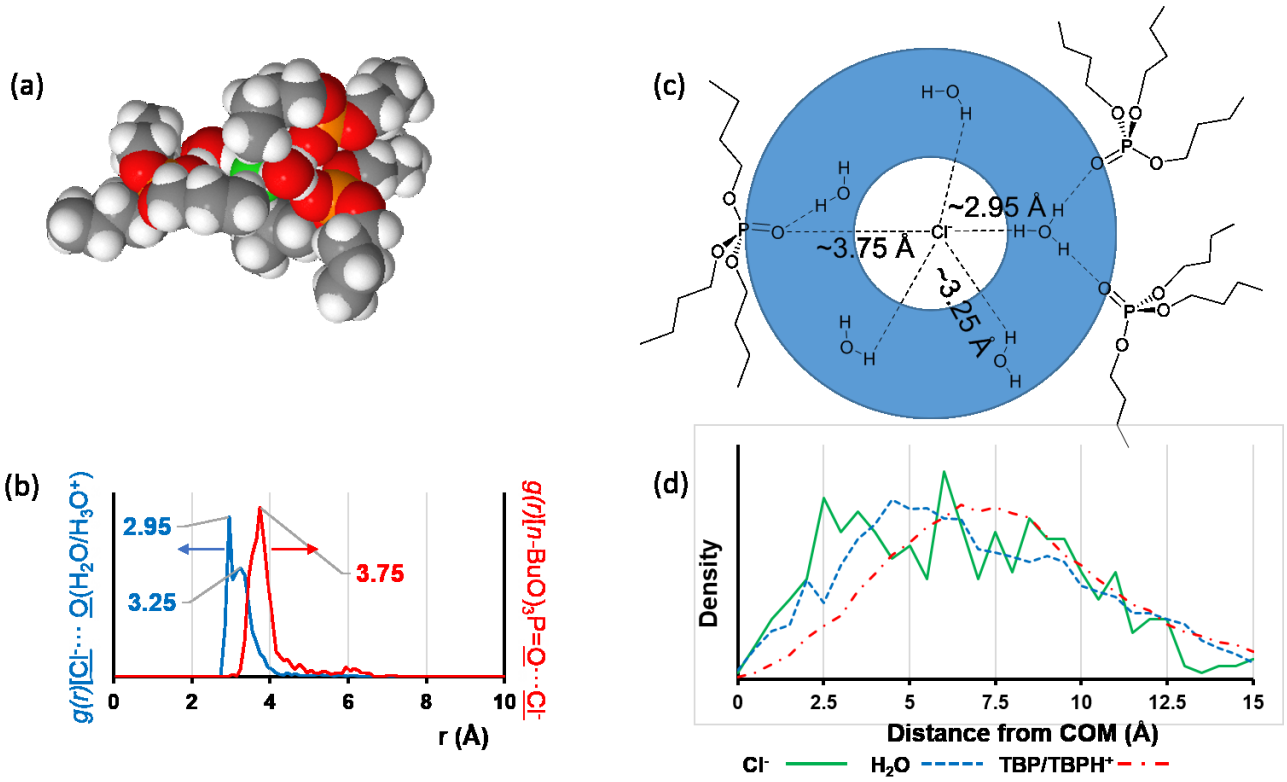

Figure 5 (a) VDW representation of aggregate formed by 3 TBP molecules around a core of $(H_2O)_4(H_3O)^+Cl^-$, (b) g(r) distance plots for the underlined atoms obtained over the production run dynamics, (c) schematic diagram showing the main structural features of the aggregate, and (d) atom probability plots showing the structure with respect to the aggregate centre of mass.

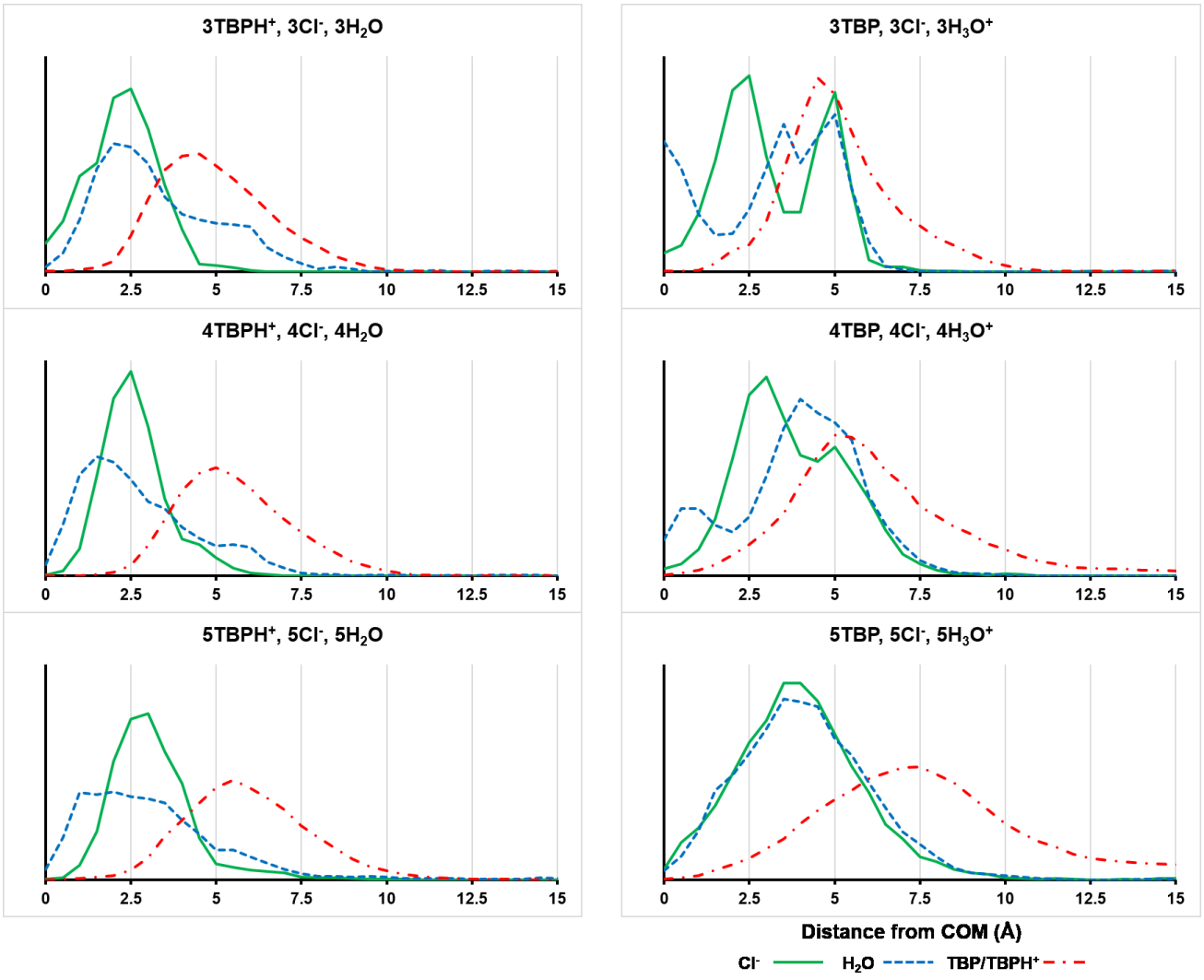

Figure 6 Atom probability plots for $(TBP.H_2O.HCl)_{3\text{-}5}$ with respect to the aggregate centres of mass with counter ions $TBPH^+$ or H_3O^+.

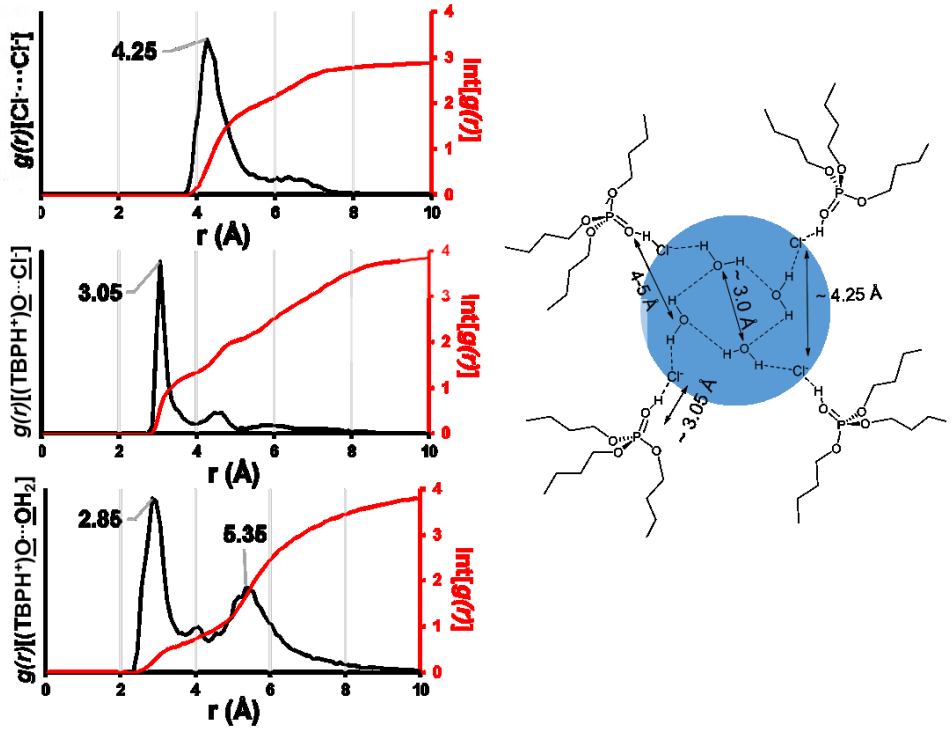

Figure 7 g(r) plots for $(TBP.H_2O.HCl)_4$ aggregates, with counter ions $TBPH^+$, obtained over the production run trajectories, with general schematic diagram highlighting the main structural details shown alongside. Integrating the g(r) plots (red lines) permit the number of interactions, as a function of distance between the denoted atom pair, to be counted.

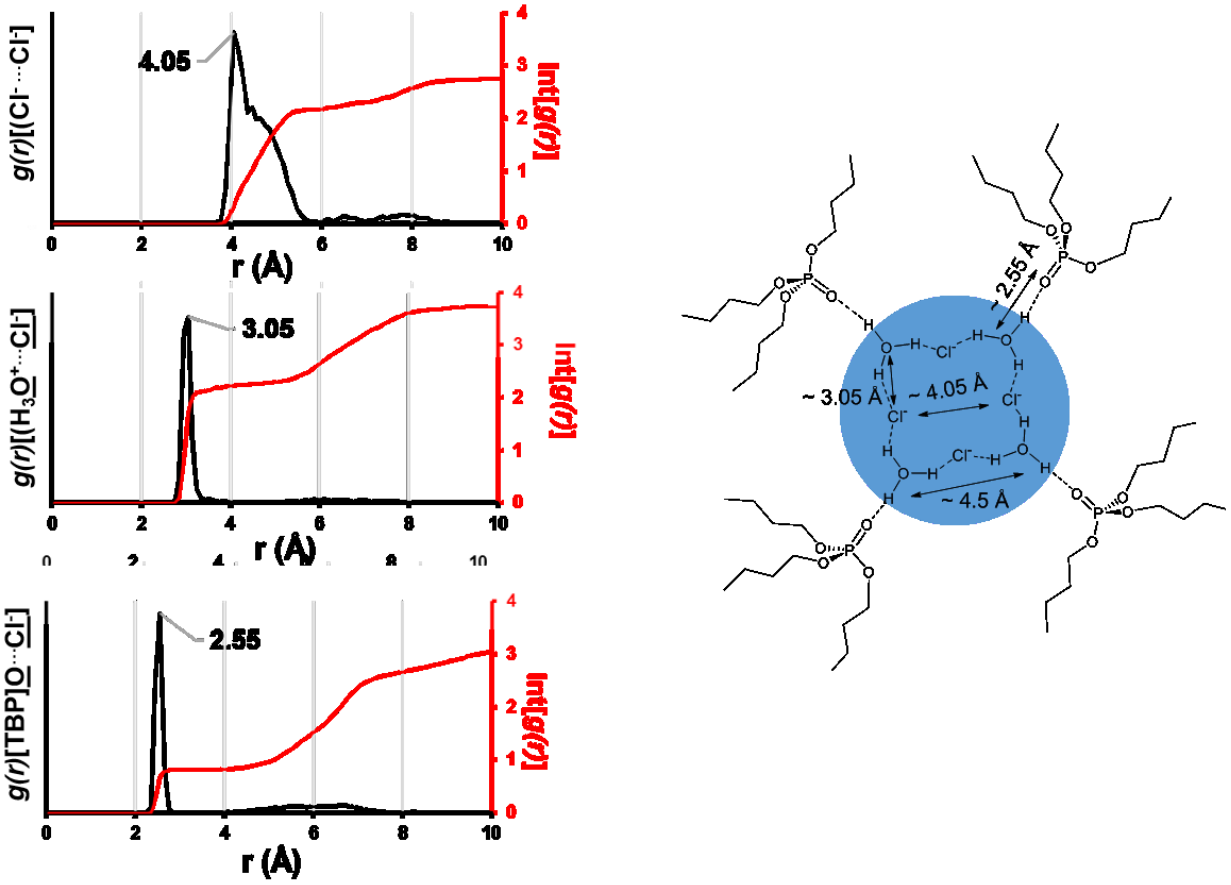

Figure 8 g(r) plots for $(TBP.H_2O.HCl)_4$ aggregates, with counter ions H_3O^+, obtained over the production run trajectories, with general schematic diagram highlighting the main structural details shown alongside. Integrating the g(r) plots (red lines) permit the number of interactions, as a function of distance between the denoted atom pair, to be counted.

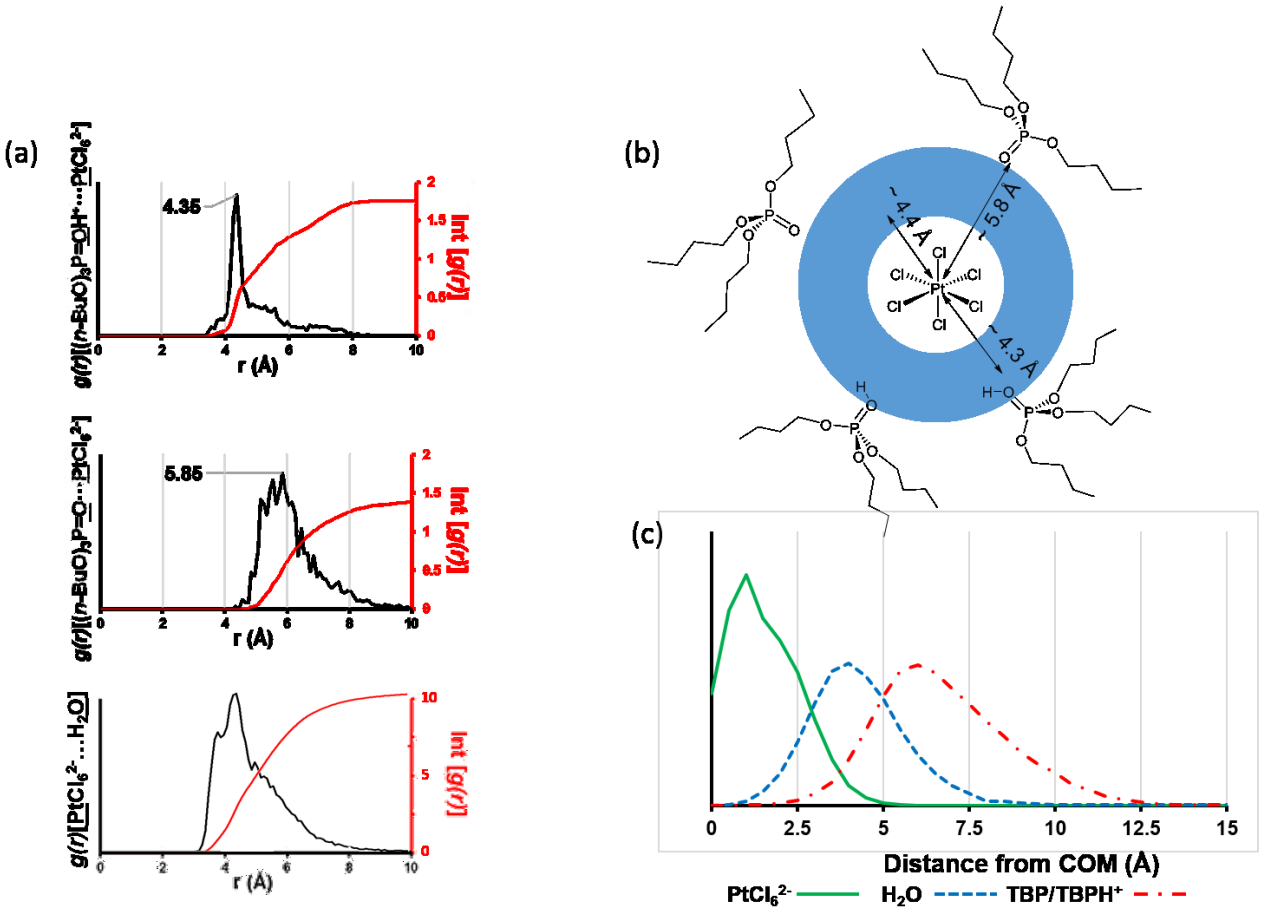

Figure 9 (a) G(r) plots for the aggregate formed by 4 TBP molecules around a core of $(H_2O)_{10}(PtCl_6^{2-})$, obtained from the production run trajectory, (b) representative structure (water molecules are contained within blue shell), and (c) atom probability plot, where the counter-ions are $TBPH^+$. Integrating the g(r) plots (red lines) permit the number of interactions, as a function of distance between the denoted atom pair, to be counted.

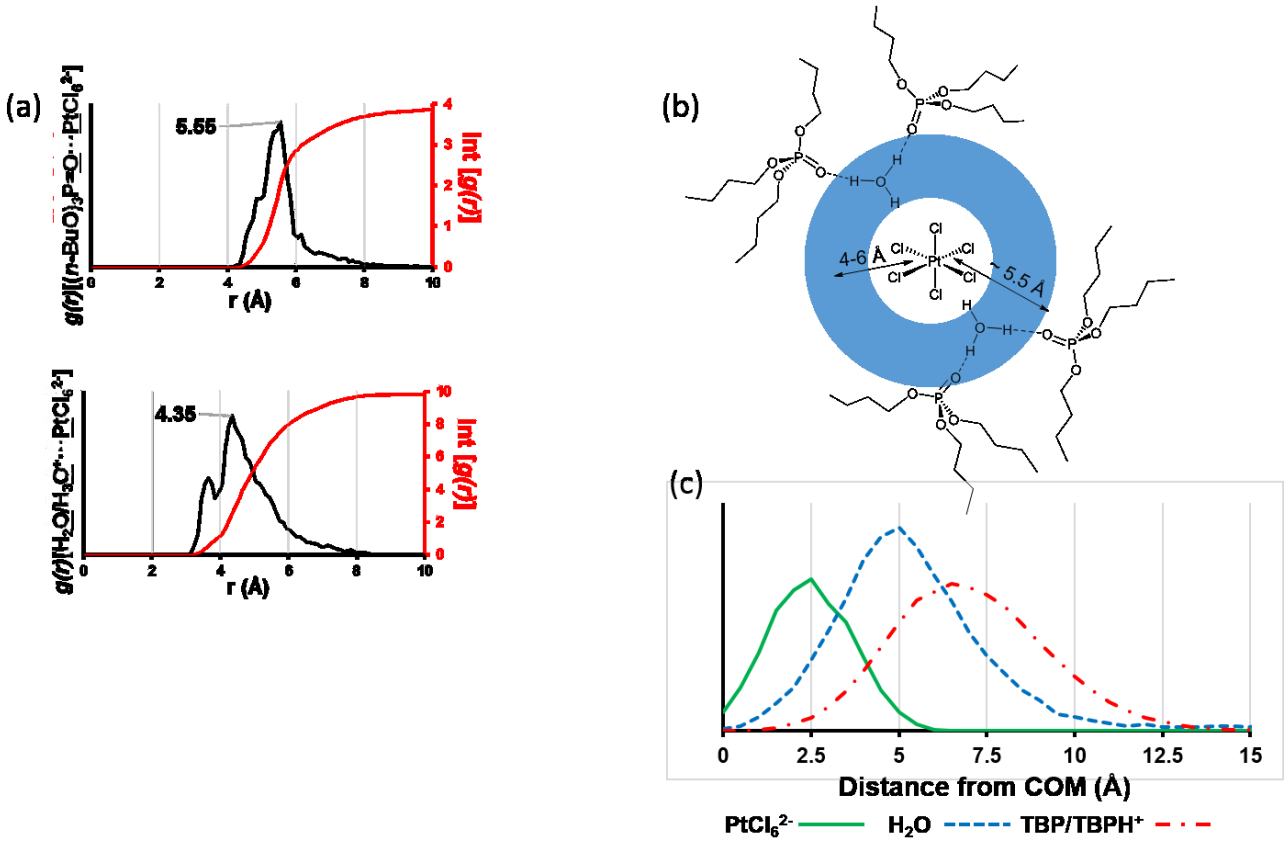

Figure 10 (a) G(r) plots for the aggregate formed by 4 TBP molecules around a core of $(H_2O)_{10}(PtCl_6^{2-})$, obtained from the production run trajectory, (b) general schematic structure (water molecules are contained within blue shell), and (c) atom probability plot. Counter-ions are H_3O^+. Integrating the g(r) plots (red lines) permit the number of interactions, as a function of distance between the denoted atom pair, to be counted.

References

1. Schulz, W. W.; Navratil, J. D.; Kertes, A. S., *Science and Technology of Tributyl Phosphate*; CRC Press: Boca Raton, FL, USA, 1984.
2. Hesford, E.; McKay, H. A. C., The Extraction of Mineral Acides by Tri-N-Butyl Phosphate (Tbp). *J. Inorg. Nucl. Chem.* **1960**, *13*, 156-164.
3. Morris, D. F. C.; Bell, C. F., The Extraction of Cobalt(Ii) at Tracer Concentration from Hydrochloric Acid Solutions into Tri-N-Butyl Phosphate. *J. Inorg. Nucl. Chem.* **1959**, *10*, 337-339.
4. Irving, H.; Edgington, D. N., The Extraction of Some Metal Chlorides into Tri-N-Butyl Phosphate. *J. Inorg. Nucl. Chem.* **1959**, *10*, 306-318.
5. Front Matter A2 - Choppin, Gregory R. In *Radiochemistry and Nuclear Chemistry (Third Edition)*, Liljenzin, J.-O.; Rydberg, J. A. N., Eds. Butterworth-Heinemann: Woburn, 2002; pp 583-641.
6. T. Nakashima; Kolarik, Z., The Formation of a Third Phase in the Simulataneous Extraction of Actinide(Iv) and Uranyl Nitrates by Tributyl Phosphate in Dodecane *Solvent Extraction and Ion Exchange* **1983**, *1*, 497-513.
7. Osseo-Asare, K., Aggregation, Reversed Micelles, and Microemulsions in Liquid-Liquid Extraction: The Tri-N-Butyl Phosphatediluent-Water-Electrolyte System. *Advances in Colloid and Interface Science* **1991**, *37*, 123-173.
8. A. V. Tatarnikov; I. Sokolskaya; Ya., M. S.; A. Yu. Lapin; Goncharov, P. M., Treatment of Platinum Flotation Products. *Platinum Metals Rev.* **2004**, *48*, 125-132.

9. F. L. Bernardis; R. A. Grant; Sherrington, D. C., A Reivew of Methods of Separation of the Platinum-Group Metals through Their Chloro-Complexes. *Reactive & Functional Polymers* **2005**, *65*, 205-217.
10. Carson, I., et al., Anion Receptor Design: Exploiting Outer-Sphere Coordination Chemistry to Obtain High Selectivity for Chloridometalates over Chloride. *Inorganic Chemistry* **2015**, *54*, 8685-8692.
11. Warr, R. J., et al., Selective Extraction and Transport of the [Ptcl6]2− Anion through Outer-Sphere Coordination Chemistry. *Chemistry – A European Journal* **2009**, *15*, 4836-4850.
12. Bell, K. J.; Westra, A. N.; Warr, R. J.; Chartres, J.; Ellis, R.; Tong, C. C.; Blake, A. J.; Tasker, P. A.; Schröder, M., Outer-Sphere Coordination Chemistry: Selective Extraction and Transport of the [Ptcl6]2− Anion. *Angewandte Chemie International Edition* **2008**, *47*, 1745-1748.
13. Ellis, R. J.; Chartres, J.; Henderson, D. K.; Cabot, R.; Richardson, P. R.; White, F. J.; Schröder, M.; Turkington, J. R.; Tasker, P. A.; Sole, K. C., Design and Function of Pre-Organised Outer-Sphere Amidopyridyl Extractants for Zinc(Ii) and Cobalt(Ii) Chlorometallates: The Role of C□H Hydrogen Bonds. *Chemistry – A European Journal* **2012**, *18*, 7715-7728.
14. Ellis, R. J.; Chartres, J.; Tasker, P. A.; Sole, K. C., Amide-Functionalized Aliphatic Amine Extractants for Co(Ii) and Zn(Ii) Recovery from Acidic Chloride Media. *Solvent Extraction and Ion Exchange* **2011**, *29*, 657-672.
15. Turkington, J. R.; Cocalia, V.; Kendall, K.; Morrison, C. A.; Richardson, P.; Sassi, T.; Tasker, P. A.; Bailey, P. J.; Sole, K. C., Outer-Sphere Coordination Chemistry: Amido-Ammonium Ligands as Highly Selective Tetrachloridozinc(Ii)Ate Extractants. *Inorganic Chemistry* **2012**, *51*, 12805-12819.
16. Narita, H.; Morisaku, K.; Tanaka, M., Highly Efficient Extraction of Rhodium(Iii) from Hydrochloric Acid Solution with Amide-Containing Tertiary Amine Compounds. *Solvent Extraction and Ion Exchange* **2015**, *33*, 407-417.
17. Wilson, A. M.; Bailey, P. J.; Tasker, P. A.; Turkington, J. R.; Grant, R. A.; Love, J. B., Solvent Extraction: The Coordination Chemistry Behind Extractive Metallurgy. *Chemical Society Reviews* **2014**, *43*, 123-134.
18. Philip Horwitz, E.; Kalina, D. C.; Diamond, H.; Vandegrift, G. F.; Schulz, W. W., The Truex Process - a Process for the Extraction of the Tkansuranic Elements Erom Nitric Ac in Wastes Utilizing Modified Purex Solvent*. *Solvent Extraction and Ion Exchange* **1985**, *3*, 75-109.
19. Osseo-Asare, K., Volume Changes and Distribution of Hcl and H2o in the Tri-N-Butyl Phosphate-H2o-Hcl Liquid-Liquid System: A Reversed Micellar Phenomenological Model. *Colloids and Surfaces* **1990**, *50*, 373-392.
20. Nave, S.; Mandin, C.; Martinet, L.; Berthon, L.; Testard, F.; Madic, C.; Zemb, T., Supramolecular Organisation of Tri-N-Butyl Phosphate in Organic Diluent on Approaching Third Phase Transition. *Physical Chemistry Chemical Physics* **2004**, *6*, 799-808.
21. R. Chiarizia; Briand, A., Third Phase Formation in the Extraction of Inorganic Acids by Tbp in N-Octane. *Solvent Extraction and Ion Exchange* **2007**, *25*, 351-371.
22. Baldwin, A. G.; Yang, Y.; Bridges, N. J.; Braley, J. C., Tributyl Phosphate Aggregation in the Precense of Metals: An Assessment Using Diffusion Nmr Spectroscopy. *J. Phys. Chem. B.* **2016**, *120*, 12184-12192.
23. Ellis, R. J.; Meridiano, Y.; Muller, J.; Berthon, L.; Guilbaud, P.; Zorz, N.; Antonio, M. R.; Demars, T.; Zemb, T., Complexation-Induced Supramolecular Assembly Drives Metal-Ion Extraction. *Chemistry – A European Journal* **2014**, *20*, 12796-12807.
24. Qiao, B.; Muntean, J. V.; Cruz, M. O. d. l.; Ellis, R. J., Ion Transport Mechanism in Liquid-Liquid Interface. *Langmuir* **2017**, *33*, 6135-6142.
25. Antonio, M. R.; Ellis, R. J.; Estes, S. L.; Bera, M. K., Structural Insights into the Multinuclear Spectiation of Tetravalent Cerium in the Tri-N-Butyl Phosphate-N-Docdecane Solvent Extraction System. *Physical Chemistry Chemical Physics* **2017**, *19*, 21304-21316.
26. Ellis, R. J.; Meridiano, Y.; Chiarizia, R.; Berthon, L.; Muller, J.; Couston, L.; Antonio, M. R., Periodic Behaviour of Lanthanide Coordination within Reverse Micelles. *Chemistry – A European Journal* **2013**, *19*, 2663-2675.
27. Reddy, T. R.; Meeravali, N. N.; Reedy, A. V. R., Reverse Micelle Mediated Bulk Liquid Membrane Separation of Platinum, Gold and Silver from Real Samples. *Separ. Sci. Technol.* **2013**, *48*, 1859-1866.

28. Qiao, B.; Demars, T.; Cruz, M. O. d. l.; Ellis, R. J., How Hydrogen Bonds Affect the Growth of Reverse Micelles around Coordinating Metal Ions. *J. Phys. Chem. Lett.* **2014**, *5*, 1440-1444.
29. R. Chiarizia; P. G. Rickert; D. Stepinski; P. Thiyagarajan; Littrell, K. C., Sans Study of Third Phase Formation in the Hcl-Tbp-N-Octane System. *Solvent Extraction and Ion Exchange* **2006**, *24*, 125-148.
30. Lum, K. H.; Stevens, G. W.; Kentish, S. E., The Modelling of Water and Hydrochloric Acid Extraction by Tri-N-Butyl Phosphate. *Chemical Engineering Science* **2012**, *84*, 21-30.
31. A. S. Kertes; Halpern, M., *J. Inorg. Nucl. Chem.* **1961**, *16*, 118-123.
32. Plimpton, S., *J. Comp. Phys.* **1995**, *117*, 1-19.
33. W. Jorgensen; D. Maxwell; Tirado-Rives, J., *J. Am. Chem. Soc.* **1996**, *118*, 11125-11236.
34. Jorgensen, W. L.; Chandrasekhar, J.; Madura, J. D.; Impey, R. W.; Klein, M. L., Comparison of Simple Potential Functions for Simulating Liquid Water. *J. Chem. Phys.* **1983**, *79*, 926-935.
35. M. J. Frisch, et al. Gaussian, Inc.. Wallingford CT, 2009.
36. S. Cui; V. F. de Almeida; B. P. Hay; X. Ye; Khomami, B., Molecular Dynanics Simulation of Tri-N-Butyl-Phosphate Liquid: A Force Field Comparable Study. *J. Phys. Chem. B.* **2012**, *116*, 305-313.
37. Schurhammer, R.; Wipff, G., Effect of the Tbp and Water on 5the Complexation of Uranyl Nitrate and the Dissolution of Nitric Acid into Supercritical Co_2. A Theoretical Study. *J. Phys. Chem. A.* **2005**, *109*, 5208-5216.
38. L. Martinez; R. Andrade; E.G. Birgin; Martinez, J. M., *J. Comput. Chem.* **2009**, *13*, 2157-2164.
39. W. Humphrey; Dalke, A.; Schulten, K., *J. Molec. Graphics* **1996**, *14*, 33-38.
40. Nosé, S., A Unified Formulation of the Constant Temperature Molecular Dynamics Methods. *J. Chem. Phys.* **1984**, *81*, 511-519.
41. Hoover, W. G., Canonical Dynamics: Equilibrium Phase-Space Distributions. *Phys. Rev,. A.* **1985**, *31*, 1695-1697.
42. P. Bach; D. Gourisse; Kikindai, T., *Bull. Soc. Chim. France* **1982**, *5-6*, I-173-I-178.
43. Kertes, A. S., Solute-Solvent Interaction in the System Hydrochloric Acid-Water-Tri-N-Butyl Phosphate. *J. Inorg. Nucl. Chem.* **1960**, *14*, 104-113.
44. Hardy, C. J., The Activity of Tri-N-Butyl Phosphate in Equilibrium with Aqueous Hydrochloric Acid. *J. Inorg. Nucl. Chem.* **1970**, *32*, 619-625.
45. P. P. Sun; J. Y. Lee; Lee, M. S., Separation of Pt(Iv) and Rh(Iii) from Chloride Solution by Solvent Extraction with Amine and Neutral Extractants. *Materials Transactions* **2011**, *52*, 2071-2076.
46. Shepherd, L. M. S.; Morrison, C. A., Simulating Proton Transport through a Simplified Model for Trans-Membrane Proteins. *J. Phys. Chem. B.* **2010**, *114*, 7047-7055.
47. Chiarizia, R.; Stepinski, D. C.; Thiyagaragan, P., *Separ. Sci. Technol.* **2006**, *41*, 2075-2095.
48. R. Chiarizia; A. Briand; M. P. Jensen; Thiyagarajan, P., Sans Study of Reverse Micelles Formed Upon the Extraction of Inorganic Acids by Tbp in N-Octane. *Solvent Extraction and Ion Exchange* **2008**, *26*, 333-359.
49. K. Huang, et al., Formation of Super-Concentrated Hydrochloric Acid in the Third Phase in Teriary Amine N235-$Ptcl_6^{2-}$-Hcl System and Its Influences in the Pt Microemulsion Extraction. *Sci China Ser B-Chem* **2009**, *52*, 1825-1834.
50. Chiarizia R.; Nash K. L.; Jensen, M. P.; Thiyagarajan, P.; Littrell, K. C., Application of the Baxter Model for Hard Spheres with Surface Adhesion to Sans Data for the U(Vi)-Hno3, Tbp-N-Dodecane System. *Langmuir* **2003**, *19*, 9592-9599.

Table of contents image

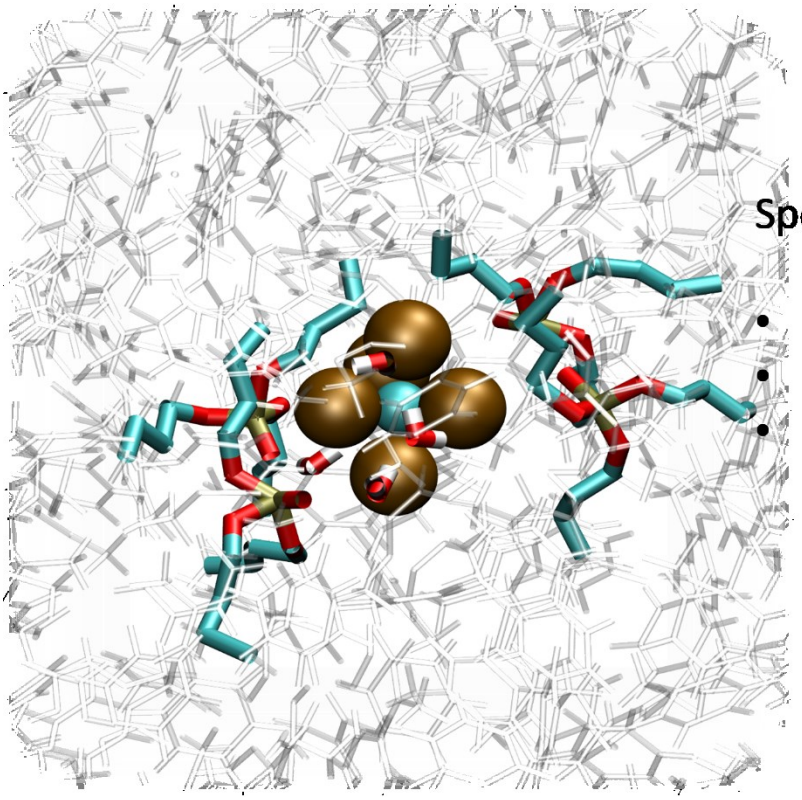

Spontaneous assembly:

- TBP encapsulating $PtCl_6^{2-}$
- mediating H_2O shell
- leaky reverse micelle structure